

**FORMATION OF CuAlO_2 THIN FILMS BY
ULTRASONIC SPRAY PYROLYSIS FOR PHOTODIODE
APPLICATIONS**

Iping Suhariadi

UNIVERSITI SAINS MALAYSIA

2011

**FORMATION OF CuAlO_2 THIN FILMS BY
ULTRASONIC SPRAY PYROLYSIS FOR
PHOTODIODE APPLICATIONS**

by

IPING SUHARIADI

Thesis submitted in fulfillment of the requirements

for the Degree of

Master of Science

August 2011

ACKNOWLEDGEMENTS

Firstly, I would like to thank to Allah SWT for His mercy enabling me to compose this thesis. May peace be upon our beloved Prophet, Muhammad SAW. I would like to thank to my main supervisor, Assoc.Prof.Dr. Zainovia Lockman for her continuous effort in supervision, encouragement and her helps when I was facing any obstacles during my research. I also like to thank my Co-supervisor, Assoc.Prof.Dr. Sabar D. Hutagalung for all of his advice and support. I would also like to thank to Prof. Kamsul Abraha for his assistance and Prof. Matsuda Atsunori for his advice regarding this research.

I would like to the thank Dean of PPKBSM Prof. Dr. Ahmad Fauzi Mohd Noor and to all academic, administrative and technical staffs of the PPKBSM for their kind assistance and supports. Especially Mr. Suhaimi, Mrs. Fong, Mr. Sahrul, Mr. Zaini, Mr. Azam, and Mr. Rashid. I would also thank to all technical staffs from Nano Optoelectronic Research (NOR) lab of the School of Physics, USM for their assistance and technical support during my MSc works.

I would like to show my deepest gratitude to AUN/SEED-Net JICA for the financial support (2009-2011). My sincere thanks to the AUN/SEED-Net JICA team, Mr. Takahashi, Ms. Siriporn, Ms. Kanchana, Ms. Karnkitti and USM international office staffs: Mrs. Irda, Mrs. Norpisah.

Many thanks to all of the Electronic Laboratory Members, P'Teguh, Kak Sya, Cheah Li, Mas Cahyo. I wish to thank to all of postgraduate students in PPKBSM USM and AUN/SEED-Net friends, Mr. Villay, Ms. Bhum, Ann, Mr. Phat, Mr. Toung,

Phanny, Lin. I also want to thanks to my Indonesian friends Bapak and Ibu Syaf, P' Shamsuddin and family, P' Subhi and Family, P' Sudibyoy, P' fathur, Niken, Alm. P' Martunus, P'Syamsiro, P'Djanter, Imam, P'Dadan, P'Tri, P'Dadan, Sunarso.

Finally, I want to take this opportunity to show my special thanks to my family, my mom and my dad. Thank you for your endless love and support. I dedicate this thesis for them.

Thank you all.

Iping Suhariadi

TABLE OF CONTENTS

	Page
ACKNOWLEDGMENTS	ii
TABLE OF CONTENTS	iv
LIST OF TABLES	viii
LIST OF FIGURES	ix
LIST OF ABBREVIATION	xiii
LIST OF SYMBOLS	xiv
LIST OF PUBLICATIONS	xv
ABSTRAK	xvi
ABSTRACT	xvii
CHAPTER 1: INTRODUCTION	
1.1 Introduction	1
1.2 Problem statement	2
1.3 Objectives of the research	5
1.4 Scope of study	5
1.5 Thesis structure	6
CHAPTER 2: LITERATURE REVIEW	
2.1 Introduction	7
2.2 Transparent Conducting Oxides (TCOs)	9
2.2.1 N-type semiconductor	9

2.2.2	P-type semiconductor	11
2.2.2.1.	Spinel Oxide	14
2.2.2.2.	Non Delafossite : Cu_2SrO_2	15
2.2.2.3.	Delafossite p-type TCO	17
2.3	Delafossite p-type CuAlO_2	18
2.4	CuAlO_2 : Phase Equilibria	22
2.5	Properties of CuAlO_2	26
2.6	Application	29
2.6.1.	Optoelectronics	29
2.6.2.	Photo electrochemical devices	33
2.7.	Synthesis of CuAlO_2	33
2.7.1.	CuAlO_2 Powder Formation	34
2.7.2.	CuAlO_2 thin film formation	35
2.7.2.1.	CuAlO_2 thin film formation by Physical Deposition Methods	35
2.7.2.1.1.	CuAlO_2 Formation by PLD	35
2.7.2.1.2.	CuAlO_2 by sputtering	36
2.7.2.2.	CuAlO_2 by solid state reaction	36
2.7.2.2.	CuAlO_2 thin film formation by chemical deposition method (CSD)	37
2.7.3.	Chemical Process via Ultrasonic Spray Pyrolysis (USP)	38
2.7.3.1.	Atomizer	39
2.7.3.2.	Temperature	42
2.7.3.3.	Aerosol Transport	46

2.8.	CuAlO ₂ Formation by Ultrasonic Spray Pyrolysis	48
------	--	----

CHAPTER 3: MATERIALS AND METHODS

3.1	Introduction	51
3.2	USP System Design	51
3.3	Chemicals	53
3.3.1	Precursor materials	53
3.3.2	Chemicals for Cleaning Process	54
3.3.3	Substrate	54
3.4	Experimental Procedures	56
3.4.1	Substrate cleaning process	56
3.4.1.1	Si wafer cleaning process	56
3.4.1.2	Glass slide cleaning process	58
3.4.2	Precursor preparation	58
3.4.3	Formation of CuAlO ₂ thin films	59
3.4.3.1	Spray pyrolysis process	59
3.4.3.2	Back contact electrode deposition	63
3.5	Characterization Techniques	64
3.5.1	X-ray Diffraction (XRD)	64
3.5.2	Field Emission Scanning Electron Microscope (FESEM)	65
3.5.3	Ultraviolet Visible Spectroscopy (UV/Vis)	66
3.5.4	Photoluminescence (PL)	67

3.5.5 Atomic Force Microscopy (AFM)	69
3.5.6 Raman Spectroscopy	69
3.5.7 Semiconductor Parameter Analysis (SPA) Meter	70

CHAPTER 4: RESULTS AND DISCUSSION

4.1 Introduction	72
4.2 USP for CuAlO ₂ Film Formation	72
4.2.1 Effect of Flow Rate of the Carrier Gas	75
4.2.2 Effects of Nozzle-Substrate Distance	88
4.2.3 Effects of Deposition Temperature	95
4.2.3.1 Physical and Chemical Properties	95
4.2.3.2 Optical Properties	106
4.2.3.3 Electrical Properties	112
4.2.4 The effect of Cu to Al ratio	125
4.2.4.1. Physical and Chemical Properties	125
4.2.4.1. Optical Properties	128
4.2.4.2. Electrical Properties	132

CHAPTER 5: CONCLUSION AND RECOMMENDATION

5.1 Conclusion	136
5.2 Recommendation for Future Research	1

REFERENCES	139
-------------------	-----

APPENDICES

LIST OF TABLES

	Page
2.1 Summary of the properties of CuAlO ₂ prepared by several techniques	50
3.1 List of chemicals used in cleaning of substrate	54
4.1 Condition parameters of spray deposition process (flow rate variation from 1L/min-4L/min)	75
4.2 Spray conditions for film deposited at various nozzle-substrate distance at two modes of deposition: continuous and non continuous.	88
4.3 Spray pyrolysis condition for substrate temperature effect investigation	95
4.4 EDX results for spray coated film at 400 °C at two points: A and B (as seen in Figure 4.13.(a-ii))	98
4.5 Energy gap of films formed at different deposition temperature	107
4.6 The electrical conductivity properties of the p-type CuAlO ₂ /n-type Si junction	115
4.7 Spray pyrolysis condition for Cu to Al ratio of 1, 1.2, and 2	125
5.1 Parameters and values of the most optimized samples	137

LIST OF FIGURES

	Page
2.1 A schematic band gap energy levels of a typical Transparent Conducting Oxide (TCO)	8
2.2 P-type of transparent conducting oxides that have been produced at the present	12
2.3 The schematic of diagram band which show the chemical interaction between oxide ion and cation with d-close shell electronic configuration	13
2.4 Atomic structure of AB_2O_4 spinel showing the position of A and B atoms around oxygen	14
2.5 Crystal structure of Cu_2O (i) and Cu_2SrO_2 (ii)	16
2.6 The concept of delafossite structures of 3R with the sequences of stacking AaBbCcAa along c-axis. For hexagonal 2H polytype, the stacking layer order is AaBbAb. The polyhedron and sphere represent BO_6 distorted octahedron and linearly coordinated A^+ cations	18
2.7 Schematic representation of $CuAlO_2$ at stoichiometric equilibrium state (a), nonstoichiometric state with surplus oxygen in the lattice site (b), and (c) nonstoichiometric state with excess oxygen in the interstitial site	20
2.8 The crystal structure of $CuAlO_2$. The layers of AlO_6 and Cu are alternately stacked along c-axis	22
2.9 TG-DTA evaluation of $CuAlO_2$	24
2.10 Thermodynamic stability of $CuO-Al_2O_3-CuAlO_2$ system at 0.21atm oxygen pressure	25
2.11 Band diagram of p- $CuAlO_{2+x}$ / n- $Zn_{1-x}Al_xO$	30
2.12 I-V characterization p-type $CuAlO_2$ / n-type Si	31
2.13 Energy band diagram of p type and n-type semiconductor before contact, during contact and at equilibrium	32

2.14	Summary of synthesis methods to produce film and bulk CuAlO ₂	34
2.15	Typical spray pyrolysis process system	39
2.16	Four types of film formed by USP: Dense layer (I), dense layer with incorporated particles (II), porous top layer with dense bottom layer (III) and fractal-like porous layer (IV)	43
2.17	processes (A-D) occurring when precursor droplets hit heated substrate	44
2.18	Formation mechanism of droplets structure during drying stages	46
2.19	interaction between droplets with the hot substrate surface	47
2.20	Droplet impact to the substrate	48
3.1	(a) schematic drawing of ultrasonic spray pyrolysis (b) the spray pyrolysis system used in the laboratory (PPKBSM, USM)	52
3.2	Flow chart of spray pyrolysis process	59
3.3	(a) mist chamber with transducer and nozzle (b) dimension of the mist chamber with nozzle	61
3.4	Bragg scattering. The constructive interference gives the pattern to the diffraction and occur when the scattered waved is an integer multiple of wavelength λ	65
3.5	Photoluminescence process of a typical semiconductor	68
3.6	Ag/n-type Si/p-type CuAlO ₂ heterojunctions formed for I-V characterization	70
4.1	Steps and processes occurring for film formation by USP	74
4.2	Low magnification SEM micrographs of CuAlO ₂ thin films deposited at variation of flow rate: 1 L/min (a), 2L/min (b), 3L/min (c) and 4L/min (d). Images on the left labeled (i) are low magnification images and labeled (ii) are the high magnification images	77
4.3	Two types of film morphologies obtained by USP: (I) dense film and (II) dense film with particulates on top	78
4.4	3D AFM images of the films sprayed at (a) 1 L/min, (b) 2 L/min, (c) 3 L/min and (d) 4 L/min (Temperature of substrate 550 °C and time of deposition was 2 min)	80

4.5	Roughness parameter of spray coated films at 1L/min to 4 L/min	81
4.6	The EDX characterization for sprayed coated film deposited at carrier gas flow: (a) 1 L/min and (b) 4 L/min.	82
4.7	Images of droplets (a) and illustration of the characteristic of droplets (b) flow leaving the nozzle to the substrate at four different flow rates	84
4.8	Five possibilities on the characteristic of droplets when colliding to the heated Si substrate	87
4.9	The SEM micrographs of CuAlO ₂ thin films deposited at nozzle-substrate distance: 1 cm (a-i), 2 cm (b-i) and 3 cm (c-i) for samples prepared using non continuous spray and 1 cm (a-ii), 2 cm (b-ii) and 3 cm (c-ii) for pulsed continuous	90
4.10	Schematic of decomposition processes of droplets at three different nozzle-substrate distances	91
4.11	XRD pattern for films formed different nozzle-substrate distance, <i>d</i> of 1 cm, 2 cm and 3 cm for non continuous mode	93
4.12	SEM micrographs at low and high magnification of CAO thin films deposited at temperature: 400°C (a-i) and (a-ii), 450°C (b-i) and (b-ii), 500°C (c-i) and (c-ii), 550°C (d-i) and (d-ii), and 600°C (e-i) and (e-ii)	97
4.13	Cross section of CuAlO ₂ deposited on Si substrate formed at temperature 550 °C	100
4.14	XRD characterization of CAO films deposited at various temperatures from 400°C to 600°C	101
4.15	Temperature dependent Raman spectra of CAO film deposited in the temperature range 450°C to 600°C	103
4.16	Normal mode parallel to hexagonal c-axis in the CuAlO ₂	104
4.17	Tauc plots for samples sprayed at different substrate's temperature: 400 °C (a), 450 °C (b), 500 °C (c), 550 °C (d) and 600 °C (e)	106
4.18	Adsorption coefficient of spray coated CuAlO ₂ films at temperature: 400°C (a), 450°C (b), 500°C (c), 550°C (d) and 600°C (e)	108
4.19	Photoluminescence spectrum of CuAlO ₂ thin film spray coated at 550°C	110
4.20	Optical transmission of spray coated CuAlO ₂ film grown at 550°C	112

4.21	J-V curve of CuAlO ₂ /Si at dark condition for sample made at different substrate's temperature	113
4.22	The turn on voltage p-type CuAlO ₂ /n-type Si	114
4.23	J-V characteristic of photodiode p-type CuAlO ₂ /n-type Si under illumination of light with power varied from 25 Watt to 100 Watt for films deposited at: 400°C (a), 450°C (b), 500°C (c), 550°C (d) and 600°C (d)	117
4.24	Photocurrent density subtracted to current at dark condition of spray coated CAO films in a junction with Si deposited at: 450°C (a), 500 °C (b), 550°C (c) and 600°C	119
4.25	J-V characteristic of photodiode p-type CAO/n-type Si deposited at 550 °C	122
4.26	The J-V characteristic of the photodiode deposited at 550 °C for dark condition and under the UV LED $\lambda= 357$ nm and P= 40 mW	122
4.27	The photodiode process in the pn junction layer	124
4.28	The XRD pattern of films deposited at three Cu to Al ratio of 1:1, 1.2:1, and 2:1	126
4.29	SEM micrographs of as grown CuAlO ₂ deposited at different Cu to Al ratio: 1:1 (a), 1.2:1 (b), and 2:1 (c). The figures labeled with (i) is low magnification SEM whilst the figures labeled (ii) on the right is high magnification SEM	127
4.30	Tauc plot of the films with Cu to Al ratio of 1:1 (a), 1.2:1 (b), 2:1(c)	129
4.31	Absorption coefficient of CuAlO ₂ films with different Cu to Al ratio	131
4.32	J-V characteristic of the spray coated CuAlO ₂ films at dark condition	132
4.33	The J-V curve of the n-Si/p-CuAlO ₂ under illumination for the film with the ratio Cu to Al: 1 (a), 1.2 (b), 2 (c). The initial J-V characterization is shown for the graph labeled with (-i-) on the left column, and after subtracted to the dark current on the right column labeled with (-ii-).	134

LIST OF ABBREVIATION

AFM	: Atomic Force microscopy
CSD	: Chemical Solution Deposition
CVD	: Chemical Vapour Deposition
EDS	: Energy dispersive spectroscopy
EHD	: Electrohydrodynamic
FESEM	: Field emission scanning electron microscopy
ITO	: Indium Tin Oxide
ICDD	: International Conference for Diffraction Data
SPA	: Semiconductor parameter analyser
LED	: Light Emitting Diode
PL	: Photoluminescence
TCO	: Transparent Conducting Oxide
TG/DTA	Thermogravimetric/Differential Thermal Analyzer
USP	: Ultrasonic Spray Pyrolysis
UV-Vis	: Ultraviolet-Visible
VBM	: Valence Band Maximum

LIST OF SYMBOLS

A	: Surface Area (cm^2)
$\%A$: Absorption
F_g	: Gravitation Force (Kgms^{-2})
F_e	: Electrical Force (Coulomb)
F_s	: Stokes Force (N)
h	: Planck constant (eV.s)
I	: Current (A)
I	: Intensity (Lux)
G	: Free Gibbs Energy
l	: Length (m)
N	: Number of Particles
μ	: Mobility ($\text{cm}^2\text{V}^{-1}\text{s}^{-1}$)
R	: Resistance (Ω)
$\%R$: Reflectance
S	: Enthalpy (Joule)
T	: Temperature ($^\circ\text{C}$)
t	: Thickness (cm)
ρ	: Resistivity (Ωm)
σ	: Conductivity (Sm^{-1})
v	: Frequency (Hz)

LIST OF PUBLICATIONS

1. Iping Suhariadi, Zainovia Lockman, Sabar D Hutagalung, Kamsul Abraha, Atsunori Matsuda. (2010) The formation of CuAlO₂ thin films by nitrate route chemical solution deposition method. Proceeding. The 3rd Regional Conference Interdisciplinary on Natural Resources and Material Engineering. October 2010. Malaysia
2. Iping Suhariadi, Zainovia Lockman, Sabar D Hutagalung, Kamsul Abraha, Atsunori Matsuda. (2010). Formation of CuAlO₂ Thin Films by Ultrasonic Spray Pyrolysis. Submitted to IOP Conference Series: Materials Science and Engineering and accepted on 29 May 2011.
3. Iping Suhariadi, Zainovia Lockman, Sabar D Hutagalung, Kamsul Abraha, Atsunori Matsuda. (2011) Formation of CuAlO₂ Films by Ultrasonic Spray Pyrolysis. Proceeding. The 1st International Conference on Materials Engineering and 3rd Regional Conference on Materials. February 2011. Indonesia

PEMBENTUKAN FILEM NIPIS CuAlO_2 MELALUI TEKNIK

PIROLISIS SEMBURAN UNTUK APLIKASI FOTODIOD

ABSTRAK

CuAlO_2 merupakan oksida jenis -p yang lutsinar. Apabila digabungkan dengan bahan jenis n, simpang p-n akan terbentuk dan boleh digunakan di dalam pelbagai aplikasi menarik optik dan elektronik. CuAlO_2 filem yang sekata, bebas daripada retakan dan homogen telah dihasilkan melalui proses pendedapan cecair kimia melalui teknik pirolisis semburan ultrasonik di atas substrat silicon jenis n yang telah dibersihkan. Prapenanda cecair yang digunakan adalah campuran $\text{Cu}(\text{NO}_3)_2 \cdot 3\text{H}_2\text{O}$ dan $\text{Al}(\text{NO}_3)_3 \cdot 9\text{H}_2\text{O}$. Parameter pendedapan yang mempengaruhi sifat-sifat filem adalah kadar aliran gas pembawa, jarak muncung-substrat, suhu substrat dan nisbah Cu kepada Al telah dikaji. Parameter yang optimum telah diperolehi untuk pendedapan filem: kadar aliran gas, 1 L/min, jarak muncung-substrate, 3 cm, suhu substrat 550 °C dan nisbah Cu kepada Al adalah 1.2:1. Aliran titisan daripada kebuk melalui muncung adalah laminar pada jarak dan kadar aliran gas pembawa ini. Pembentukan filem dicadangkan melalui tindakbalas pirolitik antara ion-ion Cu dan ion-ion Al di dalam setiap titisan apabila menghentam substrat yang panas. Imej SEM untuk sample yang optima menunjukkan filem terhasil mempunyai butiran dengan ketebalan $\sim 1.9 \mu\text{m}$. Spektroskop UV-Vis telah menunjukkan filem terhasil mempunyai jurang tenaga 3.54eV dan kelutsinaran melebihi 60 % dalam julat cahaya nampak. Kekonduksian filem adalah 0.354 Scm^{-1} . Filem menunjukkan sifat diod apabila simpang-p CuAlO_2 /-n Si dihasilkan dengan aliran voltan sekitar 0.4 V. Di bawah iluminasi cahaya nampak yang berlainan kuasa, diod menunjukkan sifat-sifat kesan fotoelektrik.

FORMATION OF CuAlO_2 THIN FILMS BY ULTRASONIC SPRAY PYROLYSIS FOR PHOTODIODE APPLICATIONS

ABSTRACT

CuAlO_2 is a p-type oxide which is transparent. When coupled with an n-type material, a p-n junction can be created and can be used in many interesting optical and electronic applications. Smooth, crack free and homogenous CuAlO_2 film was produced by chemical solution deposition process via ultrasonic spray pyrolysis (USP) technique on a cleaned n-type Si substrate. The precursor solution used was comprised of a mixture of $\text{Cu}(\text{NO}_3)_2 \cdot 3\text{H}_2\text{O}$ and $\text{Al}(\text{NO}_3)_3 \cdot 9\text{H}_2\text{O}$. The deposition parameter influences the film properties are the flow rate of carrier gas, nozzle-substrate distance, substrate's temperature and Cu to Al ratio was studied thoroughly. The optimum parameters were found for the films deposited at a flow rate of 1 L/min, nozzle-substrate distance of 3 cm, substrate's temperature of 550°C and Cu to Al ratio of 1.2:1. The flow was seen to be laminar at this distance and flow rate of carrier gas. The formation of films was proposed to be due to the pyrolytic reaction of Cu and Al ions in the droplets when the droplets impinged on the heated substrate. SEM images of the most optimum sample is consisted of uniform grains with film thickness of $\sim 1.9 \mu\text{m}$. UV-Vis spectroscopy revealed that the film have energy gap of 3.54 eV with transparency above 60 % at visible light range. The conductivity of the film was 0.354 Scm^{-1} . The film showed the rectifying nature of diode in a junction of p-type CuAlO_2 /n-type Si with turn on voltage around 0.4 eV. Under various illumination of incandescent lamp, the diode showed photoelectric effect.

CHAPTER I

INTRODUCTION

1.1. Introduction

Transparent conducting oxides (TCOs) are a class of materials which have attracted enormous attention from researchers and scientists all over the world. This material offer unprecedented range of applications for many exciting devices that requires both transparency and conductivity properties. Examples are to be used in devices like photovoltaic (Beyer *et al.*, 2007), flat panel displays (Lee *et al.*, 1997), and in light emitting and detecting photodiode (Kovac *et al.*, 2003).

As the name signifies, TCOs are materials which are transparent and electrically conducting. Finding a material with both properties is very challenging since highly conductive material tends to be metallic whilst high transparent material is often an insulator. However, several ceramic metal oxides are found to have a combination of being conductive yet transparent. TCOs which are widely used now are the n-types like $\text{In}_2\text{O}_3:\text{Sn}$, SnO_2 , Cd_2SnO_4 and $\text{Al}:\text{ZnO}$ (Banarjee *et al.*, 2003 and Choi *et al.*, 2007). P-type TCOs have also been reported especially those that are based on cuprate oxides. P-type, transparent delafossite CuAlO_2 was first reported by Kawazoe *et al.*, (1997). With the discovery of this CuAlO_2 , the realization of transparent p-n junctions for the creation of transparent semiconducting devices will be possible.

Apart from cuprate based oxides, there are not many transparent oxides which are reported to be hole conducting and at the same time transparent. In most oxides, electronegativity of oxygen 2p orbitals lead to the formation of deep valence band maximum (VBM) therefore hole are localized around the oxygen atom. Moreover hole doping is rather difficult as well. To overcome the strong localization, Kawazoe *et al.*, (1997) suggested on the modification of the energy band structures of several metal oxides to reduce the deep hole traps due to oxygen. This can be done by introducing cationic elements which have d^{10} closed shell with energy comparable to the oxygen 2p level. The closed d shell is also preferred to be used due to the coloration of open d shell which may induce the transparency of the films (Buljan *et al.*, 2001). There are several metal oxides that can be created following this band modification model. The oxides are centered on the cuprate based with CuAlO_2 as leading candidate. To date CuAlO_2 films have been made by various methods: physical and chemicals. The formation of film at low temperature using chemical methods is desired. Low temperature process is desired as it will widen the choice (even on polymer), reduce interface reaction and cost effective.

1.2. Problem Statement

Since Kawazoe *et al.* discovered p type conduction in CuAlO_2 , several studies on the stoichiometry and preparation techniques of a single crystalline CuAlO_2 have been made. Evaluation on the thermodynamics and kinetic stability of CuAlO_2 by solid state reaction of CuO and $\alpha\text{-Al}_2\text{O}_3$ annealed in air at 1200 °C shows the presence of CuAlO_2

(Kumekawa *et al.*, 2009). And, at lower temperatures, CuO and CuAl₂O₄ co-exist (Shy and Tseng., 2005). The existence of CuAl₂O₄ has also been reported in sol-gel derived film using nitrate precursor after been annealed at 800 °C (Salavati-Niasari *et al.*, 2009). CuAl₂O₄ and CuO are said to be stable at 625°C to 1100°C (Jacob and Alcock., 1975). And CuAlO₂ only can be formed at 1050-1200°C. At elevated temperature >1200°C the stable CuAlO₂ may decompose (Kumekawa *et al.*, 2009). There is only exist a small window at which CuAlO₂ can be formed. High deposition temperature limits the use and choice of substrate. Amorphous CuAlO₂ can be prepared by sputtering and the properties of the amorphous film are generally acceptable: transparency above 75 % in the visible region but with energy band gap of 1.6 eV. The room temperature electrical conductivity of the CuAlO₂ film is 0.32 Scm⁻¹ (Chattopadhyay *et al.*, 2007). Amorphous CuAlO₂ can be formed at much lower temperature.

Chemical spray deposition (CSD) process (CSD) is a versatile technique to form CuAlO₂ film on various substrates. CSD process can be done via spin coating, dip coating, and spray coating to produce the thin film. Spray coating can be done by spray pyrolysis technique. It has advantages over any physical methods are in term of simplicity and cost effectiveness. The operation of equipment is easy enough and applicable to extensive variety of precursor and substrate (Rim *et al.*, 2002). In 2005, Bouzidi *et al.*, (2005) had successfully produced a thin film CuAlO₂ by ultrasonic spray pyrolysis (USP) using chloride precursors on a glass substrate at substrate's temperature in the range of 450 to 525 °C. The amorphous CuAlO₂ films were transformed to crystalline CuAlO₂ after annealing at 570 °C. The films had band gap energy reported in

the range of 3.34 to 3.87 eV (Bouzidi *et al.*, 2005). It is known that there are several parameters in the USP which will determine the final properties of the film produced. One of them is the acidity level of the starting precursor. This effect of pH was studied and reported by Singh *et al.*, (2008) by varying the concentration of the HCl in the chloride precursors the pH was altered. Nonetheless the films produced were not very smooth, in fact were very inhomogenous (Singh *et al.*, 2008). Chloride precursor may not be the best of precursor to form smooth CuAlO₂ film. The inhomogeneity could be due to the presence of Cl₂ gas formed during the spray coating process. Prior to the report by Singh et al, Toonoka et al., (2002) investigated on the effect of chloride, alkoxide, nitrate and a mixture of these precursors to the properties of CuAlO₂ film made by CSD via dip coating. They reported on the superiority properties of the films produced by using nitrate precursor as nitrate derived films were much more crystalline, smoother and has better conductivity. To date, no work has been reported on the use of nitrate precursor for CuAlO₂ film formed by USP. Therefore, it is of interest to study the quality of films formed by USP via nitrate route.

In this work, CuAlO₂ thin films were produced by USP using nitrate precursors (nitrate route) on silicon. As mentioned nitrate precursors were used due to their advantages over the chlorides such as less aggressive and corrosive hence film formed may have much better homogeneity (Perednis., 2003). The deposition parameters were investigated aiming at the formation of coating with desired phase at lower temperature. Lower temperature process can be achieved by USP as the process occurs by ionic reactions within droplets. Having achieved an optimum CuAlO₂ films, the properties

especially the diode properties were studied. To date, not much have been reported on the diode properties of CuAlO_2 film. In this thesis, photodiode properties of transparent CuAlO_2 film on n-type silicon are presented.

1.3. Objective of the Research

The main objectives of this research are:

1. To produce CuAlO_2 films at lower temperature by USP using nitrate precursor.
2. To investigate the effect of the deposition parameters to the properties of the films especially the morphology, optical and electrical properties.
3. To characterize the diode properties of the CuAlO_2 films formed by USP on n-type Si especially under illumination.

1.4. Scope of Study

The study encompasses on the formation of p-type CuAlO_2 thin films at lower temperature by USP technique on an n-type (100) Si. The precursor was Cu and Al nitrate salts were dissolved in appropriate solvents. The deposition parameters were explored as to get an optimum condition to produce CuAlO_2 film with good coverage uniformity, and crystalline.

In this work X-Ray Diffraction (XRD) and Raman Spectroscopy were used to characterize the phase present. Scanning Electron Microscopy (SEM) and Atomic Force

Microscopy (AFM) were used to characterize the surface morphology of the films. Ultraviolet/Visible Spectroscopy (UV-Vis) and Photoluminescence (PL) were used to characterize the optical properties of the films. To assess the diode properties of the films on silicon, Semiconductor Parameter Analysis (SPA) was used under illumination. Series of experiments were also done to characterize the photo response of the CuAlO_2 on silicon.

1.5. Thesis Structure

This thesis consists of five chapters. The first chapter is on the background, problem statement, research objectives, and the scope of this study. The second chapter is on the literature review related to the research. The third chapter provides the detailed methodology of this research. The fourth chapter presents the analysis and discussion of the research findings. The fifth chapter provides the conclusion and suggestions for future work.

CHAPTER 2

LITERATURE REVIEW

2.1. Introduction

Transparent Conducting Oxides (TCOs) have attracted vast attention across the world due to its tremendous applications in realizing transparent electronics circuit for the formation of transparent devices (Ohta and Hosono, 2004). The two special features that must be accomplished in TCOs are wide energy gap (band gap) between the material's conduction and valence band and high concentration and mobility of the electrical carriers. Figure 2.1 represents an oversimplified energy band diagram of a typical TCO. The band gap energy between the valence band and the conduction band must be considerably bigger than the incoming energy of the visible light (photon). If the material exhibit this, visible photon will only pass through the material without any adsorption of the energy. The band gap of TCOs has to be greater than 3.1 eV to allow light with energy of 2-3 eV (visible red to blue light) to pass through the material (Thomas, 1997) .

However, highly transparent material is always associated with being insulating with high electrical resistance. To create a material with high electrical conductivity, free electrons are needed in the conduction band or free holes in the valence band. Free electron can be created by excitation of electrons from the valence band to the conduction band. But as mentioned, TCOs must have high energy gap and this limits the

generation or the excitation process by photon absorption. Generation due to heat energy is possible to excite electrons in the conduction band.

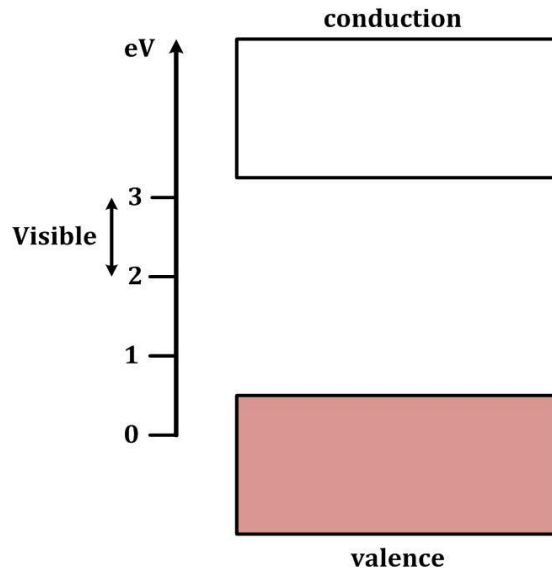


Figure 2.1: A schematic band energy levels of a typical Transparent Conducting Oxide (TCO) (Thomas, 1997)

Equation 2.1 shows the relationship of conductivity, σ with the number of free electron, N , and the mobility μ of an electron. Based on this equation, σ can be increased when N and μ are increased. N depends on the excitation process and is band gap dependent.

$$\sigma = N\mu e \quad (2.1)$$

Therefore, to reduce resistivity the carrier mobility of the carrier charge must be increased if N cannot be increased too much. As mentioned, TCOs are oxide semiconductors. The conductivity is dependent on either p or n. To get transparency, the

band gap must be > 3 eV as to allow photons with $\lambda = 300\text{-}500$ nm to transmit. Resistivity is often $\rho < 10^{-3}$ Ωcm , with degenerate carrier density $\geq 10^{20}$ cm^{-3} and the hall mobility $\mu \geq 62.5$ $\text{cm}^2\text{V}^{-1}\text{s}^{-1}$ (Calnan and Tiwari, 2010). Generation of electron or hole is dependent on intrinsic nature of the semiconductor as well. The μ is dependent on the scattering events in the semiconductor and is largely dependent on the morphology, crystallinity and impurities.

2.2. Transparent Conducting Oxides (TCOs)

2.2.1. N-Type Semiconductor

There are several n-type TCOs materials that have been used in electronic industries. They are often used as transparent electrode for optoelectronic devices. N-type TCOs have resistivity of $< 10^{-4}$ $\Omega\text{ cm}$ and overall transmittance of above 80 % at the visible photon range. Several n-type TCOs have been successfully synthesized with resistivity below 1.6×10^{-4} Ωcm , for example Al-doped ZnO (Al:ZnO) thin films deposited by pulsed laser deposition (PLD) technique (Agura, 2003). Al:ZnO produced by sputtering technique on the other hand has been reported to have resistivity of 1.39×10^{-4} Ωcm (Cao *et al.*, 2004).

Indium tin oxide (ITO) [$\text{In}_2\text{O}_3 : \text{Sn}$] is perhaps the most used n-type TCO. ITO deposited by PLD on a glass substrate has a reported resistivity value of 0.9×10^{-4} Ωcm (Choi *et al.*, 2003). ITO can also be sputtered to produce film with resistivity of $\sim 10^{-4}$ Ωcm (Ray *et al.*, 2007). However, it is believed that a shortage of indium may occur in

the near future. Moreover, the price of indium has increased drastically, thus indium free TCOs are being sought after (Minami, 2008). Moreover, indium is toxic and hence is harmful to human. Al:ZnO can be used to replace ITO as TCO for electrodes. ZnO is a material that can easily be obtained or synthesized.

Another well known n-type material is fluorine doped indium oxide (F : In₂O₃ or IFO). Thin IFO film has been reported to be produced by spray pyrolysis with resistance of 120 Ωcm and transmittance of 88 % in the visible length (Rozati *et al.*, 2004). IFO has been reported by pyrosol method with good properties to be used as electrode for solar cell (Untila *et al.*, 2009).

Recently, new semiconductor materials consist of multicomponent oxides such as ternary compounds have been produced. For example, spray coated MgIn₂O₄ film have been reported to have electrical conductivity of 0.7 Scm⁻¹ with overall transmittance of > 75 % at the visible photon range and also Hall mobility excess 1.5 x 10⁻³ cm²V⁻¹S⁻¹ (Sanjeeviraja *et al.*, 2010). Excess Mg in MgIn₂O₄ have been reported to have resulted in lowering the resistivity to 10⁻² Ωcm (Lee *et al.*, 2008). On the other hand, In₄Sn₃O₁₂ film deposited by sputtering has reported resistivity of 2 x 10⁻⁴ Ωcm, carrier concentration of ~ 10²¹ cm⁻³, Hall mobility of 20 cm²V⁻¹s⁻¹ and average transmittance of > 80% in the visible range (Minami *et al.*, 1997).

The introduction of dopant metal to a conducting binary metal oxide is well studied to achieve higher conductivity TCOs. Dopant causes disorder to the band structure of the TCOs in which will cause localization of electron in the band structures

by introducing large number of carriers (Minami, 2005). But dopants are also scattering center that may reduce μ in the TCOs.

2.2.2 P-Type Semiconductor

P-type semiconductor is characterized by the existence of acceptor level in the band energy located close to the valence band that can induce hole formation. Holes are the majority carriers responsible for the conduction mechanism of p-type materials. Among the first p-type TCOs, Sato *et al.*, (1993) reported on the NiO. However, stoichiometric NiO exhibits an electrical resistivity in the order of 10^{13} Ωcm . Its resistivity can be much lowered with the existance of nickel vacancies or interstitial oxygen. Normally, p-type conductivity is of the order magnitude smaller than in the n-type conductivity.

Apart from NiO, Cu_2O and CuO are among oxides exhibiting p-type conductivity. Figure 2.2 shows p-type TCOs materials (Banarjee *et al.*, 2008). This figure displays all of the important hole conducting TCOs and will be explained in here.

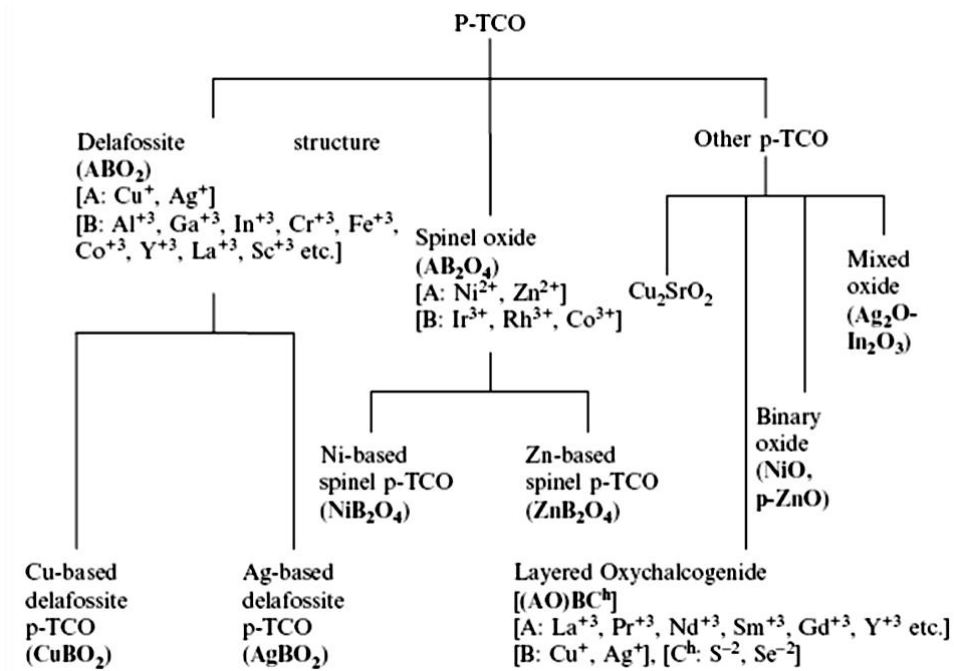


Figure 2.2. P-type of transparent conducting oxides that have been produced at the present (Banerjee *et al*, 2008).

It is best to first describe on the origin of the hole conduction in p-type TCO. As mentioned, the conductivity in p-type TCOs is much less than n-type TCOs. One of the reasons for high resistivity is on the lack of free holes available in p-type TCOs. Another reason is the mobility of holes is known to be much smaller than that of electrons. The lower conductivity of p-type is often attributed to the deep traps of highly electronegative oxygen atoms thus localizing the hole at the valence band edge of oxide. As the holes are not delocalized, they are not free to move. To overcome this problem, cation with closed d-shell can be used to create a delocalization of the holes, as shown in Figure 2.3 (Kawazoe *et al.*, 2005).

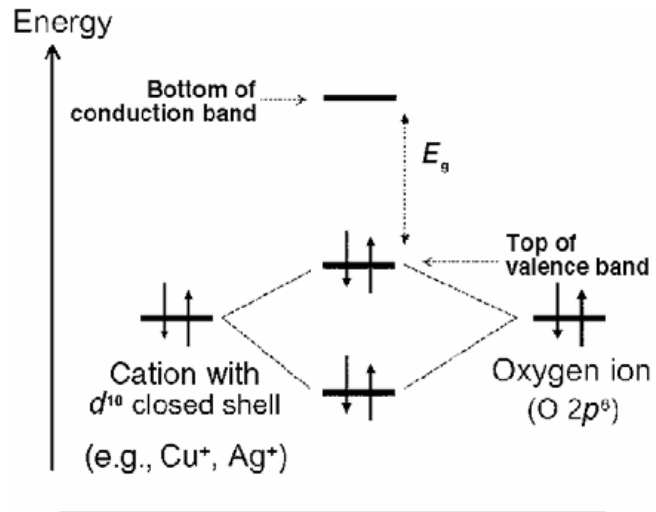


Figure 2.3. The schematic of diagram band which show the chemical interaction between oxide ion and cation with d-close shell electronic configuration (Kawazoe *et al*, 2005)

As seen in Figure 2.3, the localization from oxygen atom can significantly be reduced by the modification of the cation with d^{10} closed from the metal such as Ag and Cu. More dispersive bands with lower effective mass have been pushed up above the non bonding O 2p or Cu 3d by the interaction of metal with some O 2p state (Sheng *et al.*, 2006).

Generally there are two main p-type TCOs, that are delafossite and non delafossite oxides (Figure 2.2). The non delafossite TCOs are spinel and other types. In the other types class, SrCu_2O_2 , layered oxychalcogenide and binary oxide like NiO and mixed oxide are listed. In spinel oxide, there are Ni based and Zn based.

2.2.2.1. Spinel Oxide

The group of material known as spinel has the general formula AB_2O_4 with A is a divalent metal such as Mg, Mn, Cu, Zn, Cd, Pb, Co, Ni whereas B is a trivalent metal such as Al, Cr, Fe, Co. The structure of the spinel is given in Figure 2.4. A atoms are located at the point of a diamond type structure while the other atom are distributed around them. Each of the A atom is surrounded by four equidistant, tetrahedrally disposed oxygen atoms as shown in the Figure 2.4.i. Meanwhile, for each B atom, around them are six oxygen atom at the corner of octahedron shown in the Figure 2.4.ii. Each oxygen atom is surrounded by three equidistant B atoms and one A atom.

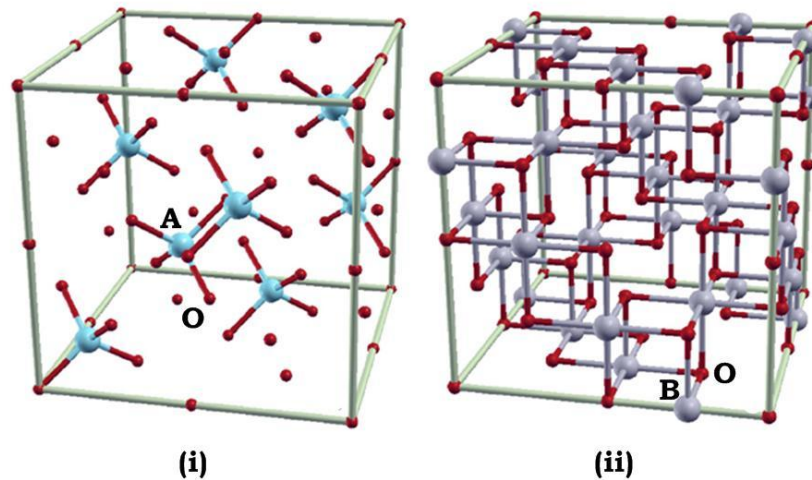


Figure 2.4. Atomic structure of AB_2O_4 spinel showing the position of A and B atoms around oxygen (Segev *et al.*, 2005)

In the spinel structure, the atomic structure is not divided into AO and B_2O_3 groups or into A and BO_2 ions. The whole crystal is a single molecule where each atom

is held by single bonds to those adjacent. Therefore, the empirical formula AB_2O_4 is the only formula which correctly represent the structure of this substance (Huggins, 1923).

The spinel $CuAl_2O_4$ thin film can be deposited by sputtering. Post heat treatment of the films increase their crystallinity. $CuAl_2O_4$ have been synthesized by sol-gel and reported to have a band gap E_g value of = 2.10 eV (Salavati-Niasari *et al.*, 2009). As seen in Figure 2.2, the p-type TCOs can be spinel oxide, Ni based or Zn based. Examples are NiB_2O_4 and ZnB_2O_4 respectively.

2.2.2.2. Non Delafossite : Cu_2SrO_2

$SrCu_2O_2$ has tetragonal crystal structure with lattice parameter of $a=5.48\text{\AA}$ and $c= 9.82 \text{\AA}$. The origin of p-type behavior in this material is resulted from +1 of Cu cation. This material can be formed at considerably low temperature and has kinetics stability (Varadarajan *et al.*, 2005). Furthermore, $SrCu_2O_2$ is built up by Cu-O chain along to the [100] and [010] direction in one dimensional, zigzag architecture with $\theta=96.3$ (Papadopoulou *et al.*, 2008).

Cu_2SrO_2 is one of a few non delafossite p-type TCOs which has a potential for optoelectronic applications (Sheng *et al.*, 2006). The crystal structure of Cu_2SrO_2 is tetragonal with space group of $I4_1/amd$ as shown in the Figure 2.5. The lattice parameters of Cu_2SrO_2 are $a= 5.48 \text{\AA}$ and $c= 9.82 \text{\AA}$ respectively. The crystal structure of Cu_2SrO_2 is consisted of Sr atoms located at the center of distorted octahedron formed by O atoms. The Cu atoms hold by O atoms to forms O-Cu-O dumbell configuration. This

dumbbell may similar to Cu_2O as shown in Figure 2.5 (i) therefore this Cu_2SrO_2 can be considered to be derived from the Cu_2O_2 . However the discrepancy of those dumbbell structure is in Cu_2O the dumbbell is built three dimensionally whilst in Cu_2SrO_2 the dumbbells arrangement is one dimensional zigzag chains along the c and b axis orientation (Nie *et al.*, 2002). Note that Cu_2O is also p-type conducting.

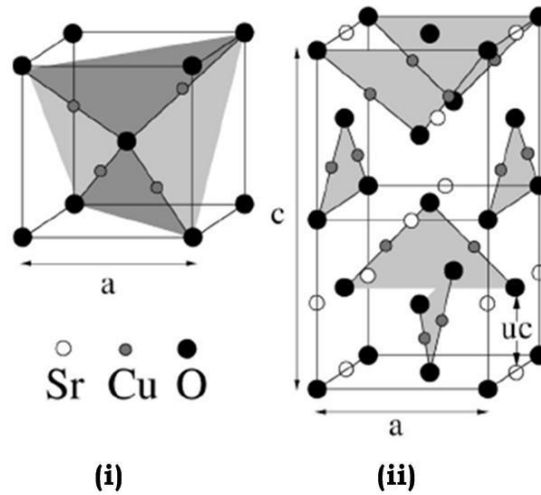


Figure 2.5. Crystal structure of Cu_2O (i) and Cu_2SrO_2 (ii)

Not many works on the synthesis of Cu_2SrO_2 have been reported so far. However, in 2003 Roy *et al* reported on the deposition of Cu_2SrO_2 thin film by spraying and PLD. The films deposited by spraying method have to be treated by post annealing in order to obtain pure Cu_2SrO_2 phase whilst the film deposited using PLD has a mixture of Cu_2SrO_2 with Cu_2O (Roy *et al.*, 2003). The improvement of Cu_2SrO_2 formation by PLD was shown by Varadarajan *et al.*, (2005) where they reported on the epitaxial growth of nearly pure phase of Cu_2SrO_2 at 500°C . MOCVD derived Cu_2SrO_2 thin film was also reported at temperature 480°C to 540°C . The as deposited film is consist of

mixture of CuO and SrCO₃ (Deschanvres *et al.*, 2008). Cu₂SrO₂ can only be synthesized at low oxygen pressure.

2.2.2.3. Delafossite p-type TCO

Delafossite has hexagonal layered crystal structure with layers of AO₂ and A stacked alternately perpendicular to c-axis. The general formula of delafossite structure is A⁺¹B³⁺O₂. As seen in Figure 2.6, delafossite consists of a rather distorted edge-shared BO₆ octahedra and closed packed A⁺ cation planes to form linear O-A⁺¹-O dumbbells. The four cations that is one A⁺¹ and three B³⁺ link the oxygen. Based on the stacking layer structures, the possible polytype may coexist are rhombohedral “3R” which have arrangement structures AaBbCcAa whilst the hexagonal “2H” polytype consists of sequence arrangement AaBbAa... (Ingram *et al.*, 2004). Nonetheless, there are no significant differences in the electrical properties between 2H and 3R since both had almost the same α -axis (Deng *et al.*, 2009).

As mentioned and seen in Figure 2.2, there two type of p-type TCOs with delafossite structures: CuB^{III}O₂ and AgB^{III}O₂ where B^{III} is trivalent cation. Ag based delafossite oxides have large band gap of > 4.12 eV and transparency above 50 % (Vanaja *et al.*, 2008). However, the Ag based delafossite is much more difficult to produce and it is unstable thermodynamically (Clayton *et al.*, 2002). The Cu based will be explained in the next sub heading.

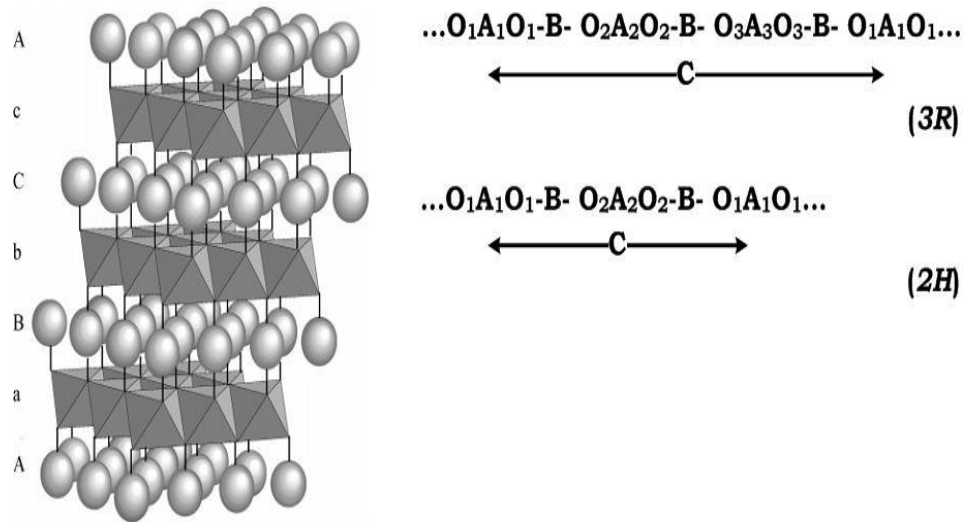


Figure 2.6. The concept of delafossite structures of 3R with the sequences of stacking AaBbCcAa along c-axis. For hexagonal 2H polytype, the stacking layer order is AaBbAb. The polyhedron and sphere represent BO_6 distorted octahedron and linearly coordinated A^+ cations (Ingram *et al.*, 2004 and Doumerc *et al.*, 1987).

2.3. Delafossite p-type $CuAlO_2$

$Cu^I M^{III} O_2$ has gained much interest as p-type TCOs. Apart from delafossite materials, Cu_2O and CuO are known to have holes conduction as well. The first report on the electrical conductivity of CuO is by Weichman where photoconductivity was reported to depend on the oxygen content in the CuO (Weichman, 1960). The energy band gap of CuO and Cu_2O are in the range of 1.7 to 2.2 eV (Kose *et al.*, 2008). The small band gap value is one of the main reason underlay CuO and Cu_2O are not being considered as TCOs. These oxides are conducting but coloured. The small band gap of Cu_2O is assumed originate from the three dimensional interaction between electron $3d^{10}$ electron and neighboring Cu^+ ions. The dumbbell unit in Cu_2O connected three

dimensionally rather than connected preferentially parallel to c-axis with two dimensional layers sandwiched by AlO_6 octahedron similar to CuAlO_2 . This controls the degree of mixing between O 2p and Cu 3d in the valence band vicinity. In Cu_2O , four Cu ion linked to each O ions. Thus, the interactions and mixing between O 2p and Cu 3d is rather smaller than those in CuAlO_2 and the valence band top of CuAlO_2 has smaller dispersion than Cu_2O . As a result the mobility and narrow gap in Cu_2O have been observed (Yanagi *et al.*, 2000). Moreover, the strong coloration effect as reported by Richardson *et al.*, (2001) which arise from the $d^{10}-d^{10}$ interaction in this copper oxides encourage many researchers to find more materials with larger band gap as to increase transparency (Buljan *et al.*, 2001).

P-type conductivity in delafossite oxides arise when there is a lack of metal cations or excess in oxygen within the crystal lattice. Defect chemistry therefore plays an important role in the determination of the final conductivity of the delafossite oxide (Koumoto *et al.*, 2001). Excess oxygen and Cu or Al deficient will create more holes as written in (2.2).



In (2.2) V_{Cu} , O_x , V_{Al} and h are Cu vacancy, oxygen in oxygen site, Al vacancy and electron hole respectively. The superscript $^{\circ}$, $'$, $''$, $*$ refer to effective charge state for neutral, negative and positive of the vacancies and holes respectively. The presence of excess oxygen in the delafossite film changes the equilibrium formula of the compound which can be rewritten as CuAlO_{2+x} . As seen in (2.2), more oxygen creates more holes.

The schematic of excess oxygen in the lattice site and interstitial site in CuAlO_2 delafossite compound is shown in Figure 2.7 (Banerjee and Chattopadhyay, 2005). In this figure, (a) shows stoichiometric CuAlO_2 whereas (b) and (c) shows excess oxygen at different sites.

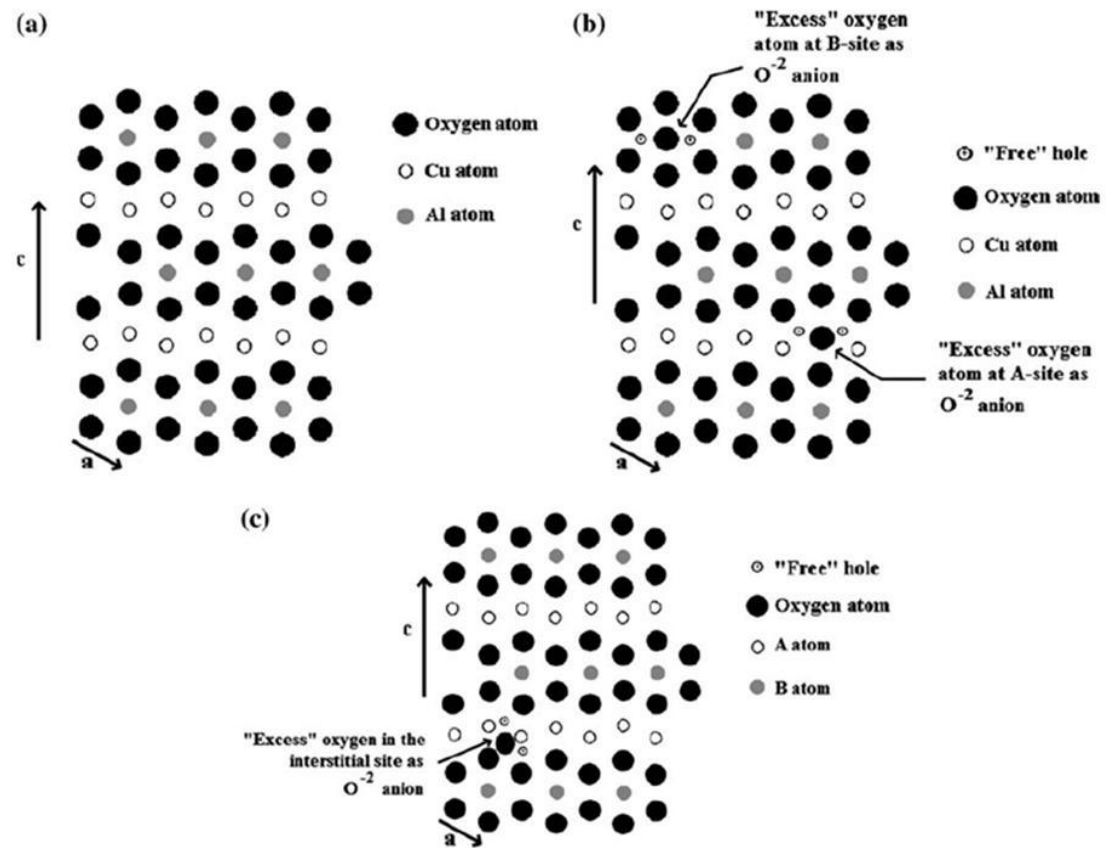


Figure 2.7. Schematic representation of CuAlO_2 at stoichiometric equilibrium state (a), nonstoichiometric state with surplus oxygen in the lattice site (b), and (c) nonstoichiometric state with excess oxygen in the interstitial site (Banerjee and Chattopadhyay, 2005)

According to Kawazoe *et al.*, (1997) most metal oxides have strong localization at the upper edge of the valence band hence no free carriers exist. The modification of the energy band structure is therefore needed as to reduce the localization and to free more carriers. To do this, the cationic species must possess a closed shell with energy comparable to the energy of the 2p levels of the oxygen anion. The Cu^+ has an electronic configuration of $d^{10}s^0$ where the energy of d^{10} closed shell will overlap to that 2p electron from the oxygen ions. The crystal structure is an important factor to be considered as well.

Tetrahedral coordination is a suitable candidate as there is a lack of oxygen bonding to the cation in the structure. This can further reducing the localization behaviors of the 2p electrons of oxide ion. In addition, lowering the dimension of crosslinking of Cu^+ ions is required to widen the bandgap because of the direct interaction between d^{10} electrons on neighbouring Cu^+ ions will reduce the band gap. As mentioned, energy gap > 3 eV must be achieved to get transparent oxide. Considering all of these requirements, Kawazoe had proposed CuAlO_2 delafossite structure one of the potential candidates for high conductive p-type TCO (Kawazoe *et al.*, 1997).

CuAlO_2 has a rhombohedral space group of R3m. In the structure, the Cu atoms are linearly linked to the oxygen atom with 2 fold coordination. Oxygens are coordinated 4-fold which comes from 3 fold by Al and 1-fold by Cu. Figure 2.8 shows the crystal structure of CuAlO_2 showing the layers of AlO_6 and Cu alternately stacked along c-axis.

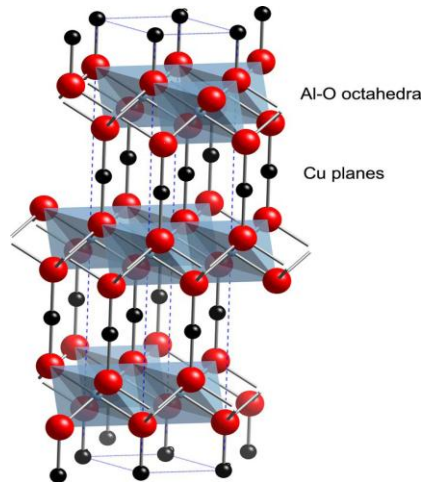
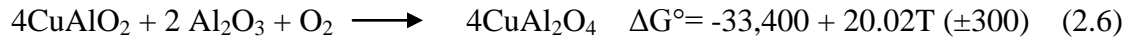
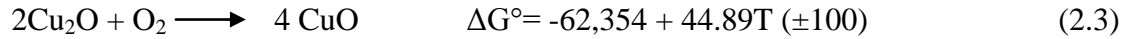


Figure 2.8. The crystal structure of CuAlO_2 . The layers of AlO_6 and Cu are alternately stacked along c -axis (Tate *et al.*, 2009).

2.4. CuAlO_2 : Phase Equilibria

As described previously, the emphasis on the p-type TCOs has been focused on gaining understanding on what is the origin of the hole conduction and how increase the conductivity. In this context, apart from crystal structure, micro structural and phase purity of p-type TCOs must also be considered. A smooth, uniform CuAlO_2 is desired to avoid electron scattering and when used in optical application, light scattering is expected in a rough oxide. Processing and formation of CuAlO_2 as p-type TCO have therefore been focused in achieving smooth, pure CuAlO_2 .

In here phase equilibria will be discussed as it is important to know on the conditions at which CuAlO_2 exist. Equations (2.3), (2.4), (2.5) and (2.6) for the formation of CuO , CuAlO_2 and CuAl_2O_4 (Jacob and Alcock., 1975).



Reactions 2.4 and 2.5 will only take place at high temperature of ~ 1100°C and 1200°C. Several works on the solid state reaction between CuO and Al₂O₃ has been reported for example Shy *et al.*, (2005). Works on Cu reaction with Al₂O₃ at temperature 1200 °C also results the formation of CuAlO₂ (Lockman *et al.*, 2009).

To study the equilibrium of CuAlO₂ phase, thermogravimetry and thermodynamic calculations have been employed. For example a mixture of CuO and Al₂O₃ followed by heating will results in the formation of CuAlO₂ by applying heat and pressure at a certain condition. The TG-DTA evaluation is shown in the Figure 2.9

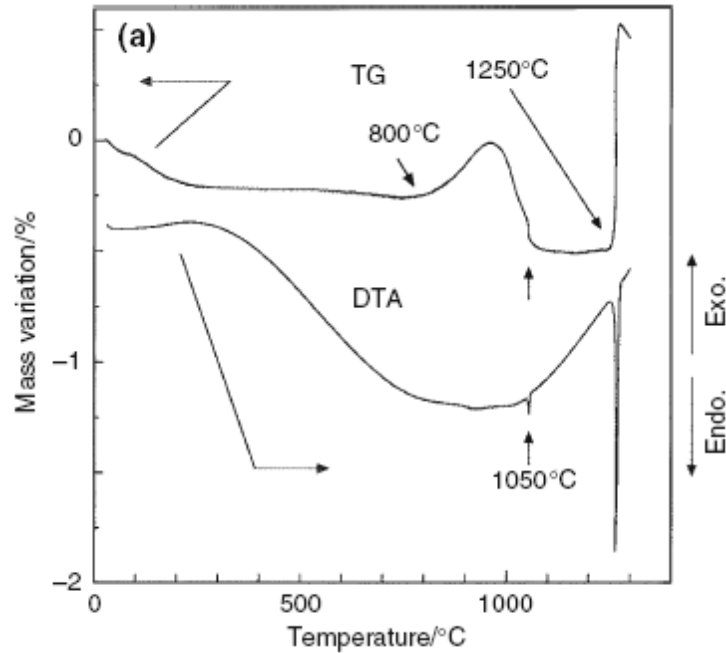


Figure 2.9. TG-DTA evaluation of CuAlO_2 (Kumekawa et al., 2009)

From Figure 2.9, the increase in mass at 800°C indicates a start of CuAl_2O_4 formation. Further heating to 950°C shows reducing of mass which indicate the formation of CuAlO_2 has started. The discontinuous mass decrease to 1050°C along with endothermic reaction attributed to the reduction of CuO converted to Cu_2O . The reaction from 1050°C to 1200°C is associated with the formation of CuAlO_2 with the reaction proposed in Equation 2.8. Furthermore, the endothermic peak at 1250°C is melting point of CuAlO_2 (Kumekawa *et al.*, 2009). The reverse reaction also is studied by Kumekawa in which CuAlO_2 powder was calcined at 900°C for about 12 hours in air. The result shows that CuAlO_2 is thermodynamically instable at temperature lower than 800°C with the reaction proposed as shown in the equation (2.7).